SITE SPECIFIC THERMODYNAMIC STUDY OF OH RADICAL ADDITION TO DNA BASES

A Thesis

Presented to

The Academic Faculty

by

Myles Akin

In Partial Fulfillment

of the Requirements for the Degree

Medical Physics in the

School of Nuclear Engineering

Georgia Institute of Technology

05/2010

SITE SPECIFIC THERMODYNAMIC STUDY OF OH RADICAL ADDITION TO DNA BASES

Approved by:

Dr. Chaitanya Deo, Advisor
School of Nuclear Engineering
Georgia Institute of Technology

Dr. Sang Cho
School of Nuclear Engineering
Georgia Institute of Technology

Dr. Chris Wang , Advisor
School of Nuclear Engineerin
Georgia Institute of Technology

Dr. David Sherrill
School of computational Chemistry
Georgia Institute of Technology

Date Approved: April 2, 2010

TABLE OF CONTENTS

LIST OF TABLES

LIST OF FIGURES

LIST OF SYMBOLS AND ABBREVIAITONS

DNA	Deoxyribosenucleic Acid
OH	Hydroxyl Radicl
DFT	Density Functional Theory
B3LYP	Becke, three parameter, Lee Yang Parr functional
BLYP	Becke Lee Yang Parr functional
PBE0	Hybrid Perdew-Burke-Ernzehof functional
6-31G**	Pople Gaussian Type basis set
$G^{\cdot}$	Guanine radical at C(5)
HOMO	Highest Occupied Molecular Orbital
LUMO	Lowest Unoccupied Molecular Orbital
FMO	Frontier Molecular Orbital theory
EP	Electrostatic Potential
G	Gibbs free energy
H	enthalpy
T	Temperature in Kelvin
S	entropy
P	electron density
χ	basis function
TNM	Tetranitromethane
TMPD	trimethyl pentanediol
NMR	nuclear magnetic resonance
GGA	generalized gradient approximation
LDA	Local Density Approximation

SUMMARY

In medical and health physics, we are interested in the effects of ionizing radiation on biological systems, in particular, human biology. The main process by which ionizing radiations causes damage to biological systems, is through the creation of radicals close to DNA strands. The radicals are very reactive and those created within close proximity to DNA will react with the DNA causing damage, in particular single strand or double strand breaks. This damage to the DNA can cause mutations that can kill the cell, either mitotically or apoptotically, or possibly lead to a cancerous formation. Therefore it is important to study how these radicals interact with DNA strands for a correlation between the resultant products of radical reactions and DNA strand breaks. For this study, we look at the most important radical, the OH radical and it's addition to DNA bases. We will study, through quantum chemistry, the thermodynamics of OH radical addition to the four bases, Adenine, Guanine, Cytosine and Thymine. The Jaguar program developed by Schrodinger was used for DFT calculations of the Gibbs free energy of the addition. In addition, calculations for the partial charge, HOMO's and Fukui indices were calculated and compared to experiment.

Chapter One

Introduction

Much work has been done toward understanding the effects of ionizing radiation on biological systems. With the increasing importance of radiation in treatment of cancer patients, medical diagnosis instruments and use of nuclear power, it is important to understand how ionizing radiation affects cells on the molecular level. Therefore knowledge of how radiation attacks DNA chemically and structurally, which are thought to be the main causes of mutagenic and lethal effects, is of great importance. Studies have shown that due to the small cross-section of DNA strands within a cell, that when irradiated, direct damage to DNA by the incident radiation is less than .5%. Radical production in the fluid surrounding the DNA strands then is the main path through which DNA is damaged by ionizing radiation, greater than 99.5%. Therefore, thorough understanding of how these radicals attack DNA strands is needed.

Ionizing radiation is radiation (photon, electrons, protons, etc.) of enough energy to detach electrons from atoms or molecules. As these particles pass through a cell, they deposit their kinetic energy in increments along their path. The measure of this deposited energy is called the Linear Energy Transfer (LET) (keV/μm) and this value depends on what type of particle is incident. Heavier charged particles have large LET while lighter particles have Low LET. This energy is deposited very close to the particle track and thus to impart energy to a target, the particle must practically hit the target. For cancer treatment, ionizing radiation is used to attack the DNA of tumor cells and thereby killing the cell through either apoptotic death or mitotic death. This is done by breaking the DNA strand and chromosome by either direct hits on the DNA strand by ionizing

particles or the creation of radicals in the aqueous solutions surrounding DNA. Radicals created within roughly 100Å of a DNA strand can then interact with the atoms within the bases or sugar phosphate backbone of the DNA strand. This interaction with the radicals will result in a radical induced product within the DNA strand. There are many different radical induced products depending on the radical reaction site (e.g. OH addition to the C(8) position on guanine can result in 8-oxo-G or FAPY-G) and each has different effects on the DNA strand. The final formation of the radical induced product depends on chemicals present within the fluid around the DNA strand. Some of these radical induced products will result in a single strand break in the DNA, a break in the sugar phosphate backbone on one side of the DNA strand. If two strand breaking products are formed in close proximity of each other, a double strand break in the DNA strand may be seen.

There are a few different radicals created in the fluid surrounding DNA including $OH^{\cdot}$, e^{aq}, and $H^{\cdot}$. Of these it is proposed that the hydroxyl radical ($OH^{\cdot}$) is perhaps the most important in DNA damage [1]. This radical may bond to or remove hydrogen atoms from DNA bases or the sugar backbone. There have been many experimental studies to identify the forms of hydroxyl radical base damage (some of which will be discussed in the literature review section) and relative amount of radical induced products. However, the reliability of these measurement has been questioned due to artifacts of the techniques used [2].

Theoretical studies of radiation damage to DNA strands had been mostly in the form of monte carlo simulations. For most of these studies, a model DNA strand is created in a solvent then irradiated. The radiation particles are simulated using particle track calculations through the solvent (typically water). The probability for damage to the DNA strand is calculated by the proximity of the energy deposition to the DNA strand and the amount of energy deposited. The closer to the DNA strand of the more energy

deposited increase the probability for damage. A more recent study by Aydogan performs a monte carlo simulation of the water radicals around a DNA strand and allows them to react with DNA strands as well as free bases. This study will be discussed in the literature review portion in this paper [4]. A more accurate picture may be produced by combining these techniques. Instead of the probability of a strand break being determined by the energy deposition from track structure calculations, the energy depositions may be used to model the creation of water radicals. These water radicals can then be allowed to interact with DNA molecules with reaction preferences given to certain bases, atoms on the bases and the sugar phosphate backbone based on favorability calculations such as the ones performed here. The resulting radical reactions with the DNA strand can then be allowed to form the radical induced products within the DNA strand. Information on the ability of the radical induced products to break DNA strands can then be used to determine the number of single strand breaks and double strand breaks. One step to this modeling then must be the determination of which bases and atoms are more favorable for interaction with water radicals. This study focuses on the OH radical with addition reaction to DNA bases.

Chapter Two

Theory

DFT

Density Functional Theory is a quantum mechanical theory used to investigate the electronic structure of many body systems, in this case molecules and atoms. It is based on the proof by Hohenburg and Khon that the ground state electronic energy is determined by the electron density ρ. Note here that the theory is based on functionals, which produces a number from a function which depends on variables. Intuitively, the proof was described by E.B. Wilson as (taken from *Intro to Comp Chem,* Jensen[8]):

- The integral of the density defines the number of electrons
- The cusps in the density define the position of the nuclei
- The heights of the cusps define the corresponding nuclear charge

The goal of the DFT method then, is to design functionals that connect the energy with the electron density.

As this is used as method to solve the many body electronic structure problem in quantum mechanics, it is derived from the many electron Schrödinger equation for a wave function Ψ.

$$\hat{H}\Psi = \left[\hat{T} + \hat{V} + \hat{U}\right]\Psi = E\Psi$$

Where $\hat{H}$ is the electronic molecular Hamiltonian, $\hat{T}$ is the electron kenetic energy, $\hat{V}$ is the potential energy from an external field and $\hat{U}$ is the electron-electron interaction energy. Formally, this can be written as

$$\hat{H}\Psi = \left[\sum_{\mathrm{i}}^{\mathrm{N}} -\frac{\hbar^2}{2\mathrm{m}}\nabla_{\mathrm{i}}^2 + \sum_{\mathrm{i}}^{\mathrm{N}} \mathrm{V}(\vec{\mathrm{r}}_{\mathrm{i}}) + \sum_{\mathrm{i}<j}^{\mathrm{N}} \mathrm{U}\left(\vec{\mathrm{r}}_{\mathrm{i}}, \vec{\mathrm{r}}_{\mathrm{j}}\right)\right]\Psi$$

Here N is the total number of electron and $\vec{\mathrm{r}}_{\mathrm{i}}$ is the location of the ith electron. Because of the electron-electron interaction, this equation is no longer separable. There a many methods to solve this problem, the simplest being the Hartree Fock method, which is not very accurate, and some of the most accurate being the post-Hartree Fock methods such as coupled cluster. However these are very computationally costly methods and are difficult to apply to larger systems. DFT offers a methods that is low in computational cost but still quite accurate in its results.

In DFT theory, the many-electron equation is now represented by functional of the electron density ρ

$$E[\rho] = T[\rho] + E_{ne}[\rho] + E_{ee}[\rho]$$

With E_{ne} being the nuclei-electron attraction and E_{ee} is the electron-electron interaction term. The E_{ee} term can be broken down further to the coulomb interaction term J[ρ] and an exchange term K[ρ]. However, the kinetic term has only a poor representation as a functional. In an attempt to fix this, Kohn and Sham introduced orbitals into DFT to allow for inclusion of the Hartree-Fock kinetic energy. This introduction of orbitals leads to the density being represented as

$$\rho = \sum_{i=1}^{N} |\emptyset_i|^2$$

With N the number of electrons and $\emptyset_i$ is the orbital of the ith electron. The kinetic energy term then is

$$T[\rho] = \sum_{i=1}^{N} \left\langle \emptyset_i \left| -\frac{1}{2}\nabla^2 \right| \emptyset_i \right\rangle$$

This introduction of orbitals requires the use of basis set expansions of the orbitals in DFT calculations. A good discussion of basis sets can be found in *Intro. to Comp. Chem.* by Jensen, Ch. 5. The main basis set used in this paper is the Pople 6-31G**. This is a split valence basis with the inner part being a contraction of 3 primitive Gaussian type oribitals (PGTO) and the outer part being one PGTO. The ** represents two sets of polarization functions.

The Khon-Sham theory calculates kinetic energy with the assumption that electrons do not interact with one another. This however, is not true and while this theory is very accurate, it does not provide 100% of the kinetic energy. The difference between the exact kinetic energy and the kinetic energy calculated by the KS term is absorbed into a new exchange-correlation term. However, the exact exchange-correlation functional is not known. The difference then between functional is the choice of the exchange-correlations term. There are a few different types of exchange-correlation functional such as Local Density Approximation, Gradient Corrected methods, Hybridmethods, etc. For an overview of these different methods see *Intro to Comp Chem* by Jensen, pg. 246-255. This study used the B3LYP and PBE0 hybrid functional and the BLYP GGA functional [5-7].

Gibbs Free Energy

Free energy, or Gibbs free energy, is a thermodynamic quantity developed by J. Willard Gibbs. The definition of this free energy is given by the equation

$$G = H - TS$$

Where G is the free energy, H is the enthalpy, T is the temperature in Kelvin and S in the entropy. Enthalpy is defined as the internal energy of a system plus the product of its volume and pressure. Entropy is a measure of the disorder of the system. For a chemicals reaction, the change in free energy is the important quantity, so the equation of interest is

$$G_{product} - G_{reactants} = \Delta G = \Delta H - T\Delta S$$

From this quantity, it can be known whether a reaction will occur spontaneously or not. If $\Delta G > 0$ then the reaction is non spontaneous, if $\Delta G < 0$ the reaction is spontaneous and if $\Delta G = 0$ the system is in equilibrium. For thermodynamically controlled reactions, the reaction with the smallest value of ΔG is the most thermodynamically favored and stable of the reactions.

HOMO/LUMO

Frontier Molecular Orbital theory [8] was developed to provide a qualitative view of reactivity based on the properties of reactants. The energy change in the reaction is estimated via perturbation theory for two atoms A and B in the two interacting molecules, is the equation

$$\Delta E = -\sum_{A,B}^{atoms} (\rho_A + \rho_B)\langle\chi_A|\boldsymbol{V}|\chi_B\rangle\langle\chi_A|\chi_B\rangle + \sum_{A,B}^{atoms} \frac{Q_A Q_B}{R_{A,B}} + \left[\sum_{i\in A}^{\substack{Occ\\MO}}\sum_{a\in B}^{\substack{Vir\\MO}} + \sum_{i\in B}^{\substack{Occ\\MO}}\sum_{a\in A}^{\substack{Vir\\MO}}\right] \frac{2(\sum_{\alpha}^{AO} c_{\alpha i} c_{\alpha a} \langle\chi_{\alpha i}|V|\chi_{\alpha a}\rangle)^2}{\varepsilon_i - \varepsilon_a}$$

The ***V*** operator contains all the potential energy terms for both of the reactant molecules. The first term is negative and represents the repulsion between occupied orbitals, the second term represents an attraction or repulsion between charged parts of the

molecules and the third term represents mixing of occupied MOs in one molecule with unoccupied (virtual) MOs on the other molecule. The largest contribution to the double summation comes from the Highest Occupied Molecular Orbit (HOMO) and the Lowest Occupied Molecular Orbit (LUMO). FMO theory considers only these contributions. From the HOMO and LUMO, the selectivity of nucleophilic and electrophilic reactions can be rationalized. The atom or site that has the largest HOMO coefficient will be the preferred site for electrophilic attack whereas the site with the largest LUMO value will be preferred for nucleophilic attack. Given this, the HOMO surfaces were calculated and the surface with the larger value (visually, the larger orbit) should be the site of preferred addition.

Mulliken Population

Of interest when studying the reaction involving an electrophilic reactant such as the $OH^{\cdot}$ radical is the distribution of partial charge over the molecule. The site that has the most negative charge, depending on the speed of the reaction, could be preferred over a less negative site, provided both a thermodynamically allowed. One method of finding the distribution of partial chare is by Mulliken Population Analysis. This method is based on the electron density at a certain position r from a single molecular orbital. This contribution to the density by the molecular orbit is given by $\rho_i(r) = \phi_i^2(r)$. Since this molecular orbit is expanded in a set of normalized basis functions (see above), ϕ_i^2 can be written as

$$\rho_i(r) = \phi_i^2 = \sum_{\alpha\beta}^{M} c_{\alpha i} c_{\beta i} \chi_\alpha \chi_\beta$$

The total number of electrons is the found by integrating and summing over all the occupied molecular orbitals.

$$\sum_{i}^{N_{occ}} \int \phi_i^2 dr = \sum_{i}^{N_{occ}} \sum_{\alpha\beta}^{M} c_{\alpha i} c_{\beta i} S_{\alpha\beta} = N_{elec}$$

Where $S_{\alpha\beta}$ is the overlap matrix of the basis functions. This can be generalized by introducing an occupation number n_i for the occupied orbital (0,1,2) as follows

$$\sum_{i}^{N_{occ}} n_i \int \phi_i^2 dr = \sum_{i}^{N_{occ}} \sum_{\alpha\beta}^{M} n_i c_{\alpha i} c_{\beta i} S_{\alpha\beta} = \sum_{i}^{N_{occ}} D_{\alpha\beta} S_{\alpha\beta} = N_{elec}$$

The Mulliken Population Analysis method uses this matrix, **D·S**, to distribute charge over the atoms in the molecule. The diagonal elements are the number of electrons in the atomic orbital and the off diagonal is half the number of electrons shared by atomic orbitals. The contributions from all atomic orbitals may be summed up for a given atom to find the number of electrons associated to that atom. Then the contribution by the basis functions on different atoms are divided equally to between the atoms. Thus, the Mulliken population and charge are defined by

$$\rho_{atom} = \sum_{\alpha \in atom}^{M} \sum_{\beta}^{M} D_{\alpha\beta} S_{\alpha\beta}, \quad Q_{atom} = Z_{atom} - \rho_{atom}$$

Fukui Function

Reactions generally involve a change in electron density, which can be represented by the Fukui Function given by

$$f(r) = \frac{\partial \rho(r)}{\partial N_{elec}}$$

This function is indicative of the change in electron density ($\rho(r)$) at a given position when the number of electrons (N_{elec}) is changed. This function is defined for either an

electrophilic or a nucleophilic reaction, i.e. the removal or addition of an electron. These are defined by

$$f_+(r) = \rho_{N+1}(r) - \rho_N(r)$$

$$f_-(r) = \rho_N(r) - \rho_{N-1}(r)$$

With a radical reaction defined by the average of f_+ and f_-. These functions when evaluated a known as the Fukui Indices. Given this, the larger the value of f_-, f_+ or the radical index, the more preferred the site of attack is. For the purpose of this paper, the radical and electrophilic Fukui indices are calculated. [8-10]

Chapter Three

The Hydroxyl Radical

The main process by which the hydroxyl radical is produced is through the following reactions

$$H_2O + ionizing\ rad. \rightarrow H_2O^{\cdot +} + e^-$$

$$H_2O^{\cdot +} \rightarrow OH^{\cdot} + H^+$$

The hydroxyl radical is very reactive and electrophilic and reacts at close to diffusion control rates [11]. For the DNA bases, the reaction rates are shown in Table 1 [12,13]. The main types of reactions $OH^{\cdot}$ undergoes are addition to the C-C and C-N double bonds, H-abstraction and Electron Transfer (ET). For the purposes of this paper, only additions to double bonds are considered with some discussion of H-Abstraction with Thymine only [4].

Table 1: Reaction rate constant for OH addition to DNA bases [$mol^{-1}\ s^{-1}$]

Reaction Rate Constants	
Thymine	$6.3x10^9$
Cytosine	$6.4x10^9$
Adenine	$6.1x10^9$
Guanine	$9.2x10^9$

The electrophilic $OH^{\cdot}$ reacts readily with C-C and C-N double bonds at close to diffusion controlled rates, but is very regioselective due to its electrophilic nature, choosing the more electron rich atom [11]. The other bond to consider within DNA bases are the C-O double bond. $OH^{\cdot}$ does not add to this bond as it is electron poor at the

carbon atom, the place $OH^{\cdot}$ would prefer to add due to the electronegativity of the atoms. Recent studies have shown through pulse radiolysis that a short lived π-complex may be formed prior to $OH^{\cdot}$ fixation, and that the pronounced regioselectivity of the hydroxyl radical may occur at the transition from π- to σ- complex [14]. Though this π-complex is a reversible reaction, once the σ-complex is formed, the radical remains tightly bound.

Of less importance in the study of DNA bases is H-abstraction, which is only seen in significant quantities in studies of Thymine. Here the removal of a hydrogen from the C(5) methyl group is seen in about 5-10% of the reactions [2,4]. Studies have been done on the thermodynamic favorability of this reaction [15] and will be presented with the discussion of Thymine. H-abstraction has shown no importance in any other DNA base.

Chapter Four

Literature Review

Experimental

For both of the pyrimidine bases, the $OH^{\cdot}$ radical adds to the C(5)-C(6) double bond and to a limited extent on Thymine, H-abstraction at the C(5) methyl group occurs.

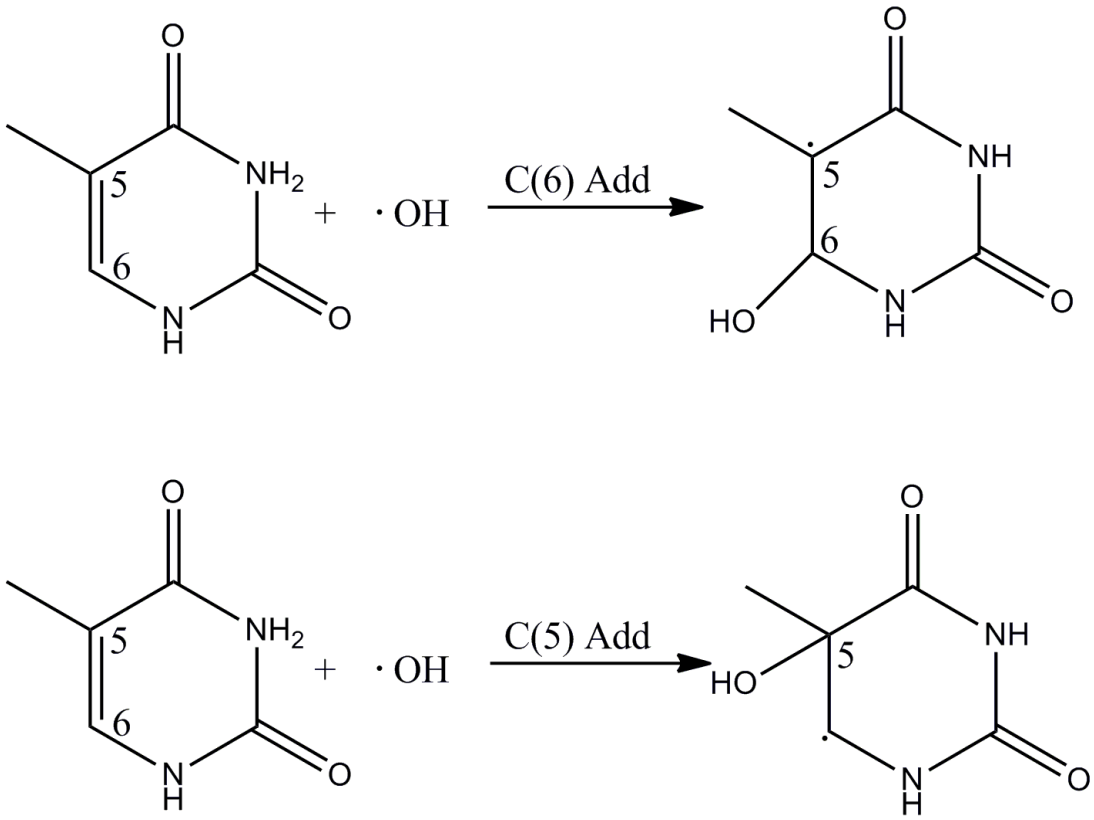

Figure 1: Hydroxyl radical addition to thymine.

When $OH^{\cdot}$ adds to the C(5) position, a new radical is formed at the C(6) atom (EPR studies done by Schulte-Frohlinde and Hildebrand 1989[16]; Catterall et al 1992[17]), these are seen in Figure 1. This radical has reducing properties due to interactions with the neighboring nitrogen atom and in pulse radiolysis studies, yield is determined by its reaction with Tetranitromethane (TNM). The reaction with TNM results in a strongly

absorbing nitroform anion which is measured. For C(6) addition, a radical with oxidizing properties is created at the C(5) position. The yield of this radical is determined with use of a reductant, usually trimethyl pentanediol (TMPD). The H-abstraction reaction gives a radical that is neither oxidizing nor reducing, therefore it is common to use the difference in the results of C(5) and C(6) addition with that of the expected yield. This however is not exact and can only give a rough estimate of the amount of H-abstraction that occurs.

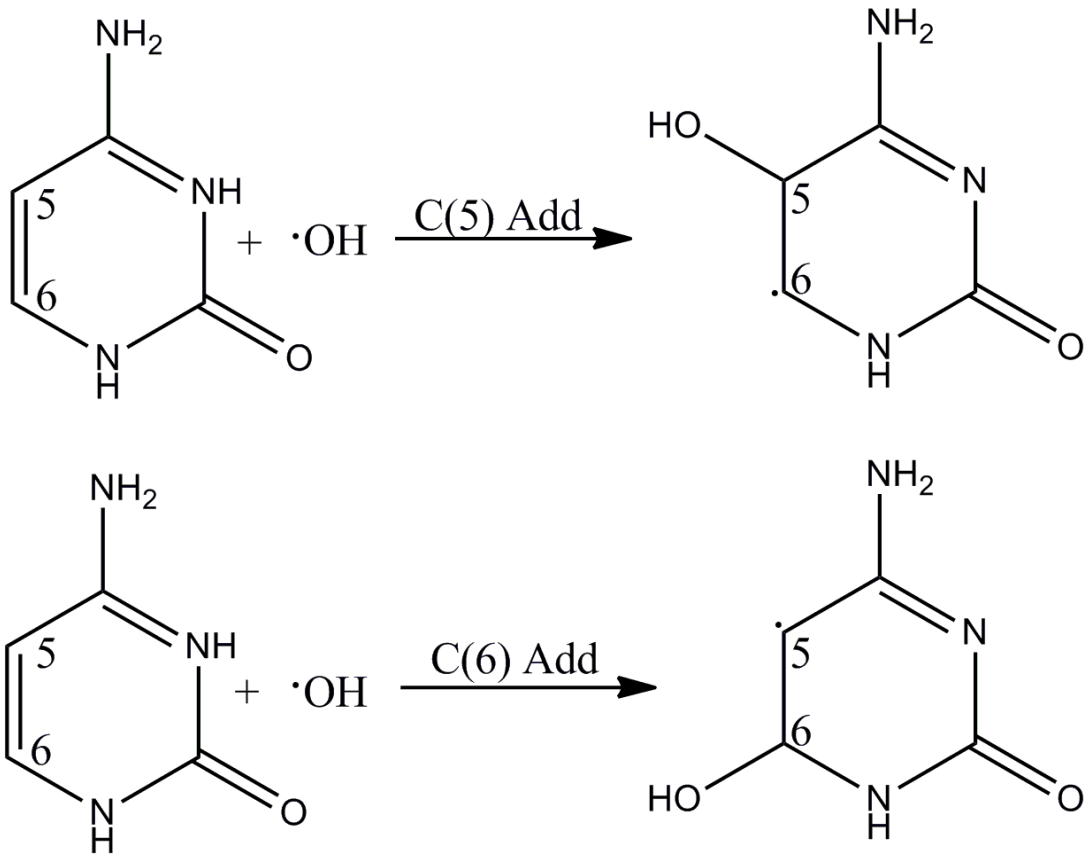

Figure 2: Hydroxyl radical addition to cytosine

For thymine in particular, the bulk of studies have used of thymidine in an aerated aqueous solution with NMR and mass spectroscopy used for analysis [2]. These studies have led to the conclusion that for thymine, the C(5) position is favored with roughly 60% of $OH^{\cdot}$ addition, C(6) with addition of around 30-35% and H-abstraction of around 5-10%. The addition reactions are shown in Figure 1. For this study, only the

addition reactions are considered. Information on cytosine is a bit lacking compared to thymine, however in studies by Steenken and Harza [18] have shown roughly 87% addition to the C(5) position and 10% addition to the C(6) site, with no data on H-abstraction. Reactions are shown in Figure 2.

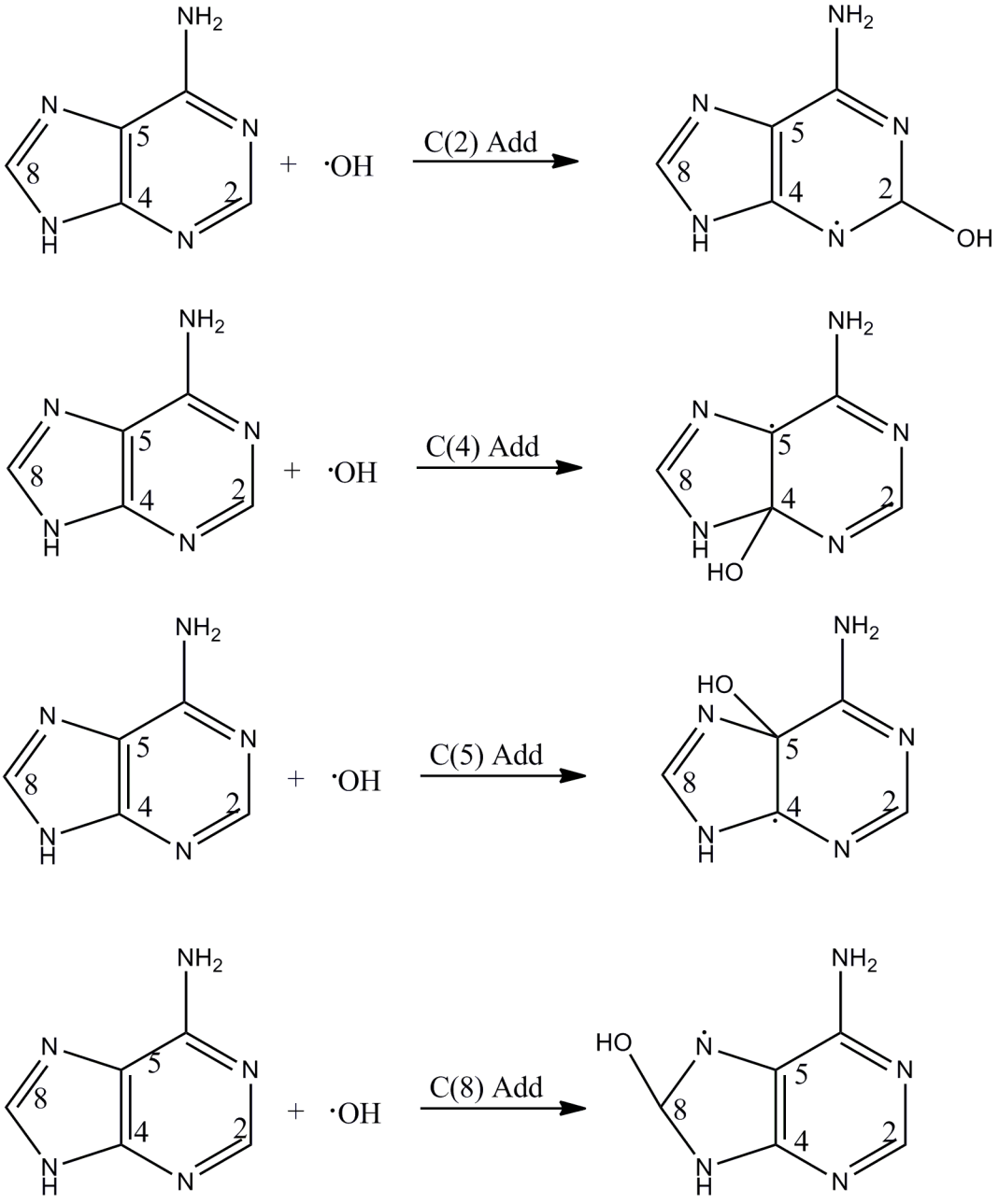

Figure 3: Hydroxyl radical addition to adenine

The purine base Guanine has the highest affinity for reaction with the $OH^{\cdot}$ radical, as can be inferred from its reaction rate constant. As such, it is the base with the most studies published and most information available. The hydroxyl radical adds to the C(2), C(4), C(5) and C(8) positions on the guanine base, as well as adenine. Addition to any of these atoms creates a radical, as seen in Figures 3 and 4. Of these radicals, it is thought that most have oxidizing properties [19-21]. One such radical is the $G^{\cdot}$ radical, which is water eliminating, and thought to be a result of C(4) addition [12]. This is shown in Figure 4. Yield of the C(4) addition is between 60-70%. From C(8) addition, a reducing radical is formed and from its reaction with $Fe(CN)_6$, it thought to have a yield of 17-25% [22]. There is no clear percentage yield for C(2) or C(5) addition to guanine. Experimental results on these two sites range from 1.5-10% for C(2) and 5% or less for C(5). The is very little information regarded hydroxyl radical addition to Adenine. From what exists [23,24], the yields for addition to adenine are 37% to C(8), 50% to C(4) and less than 5% for C(5).

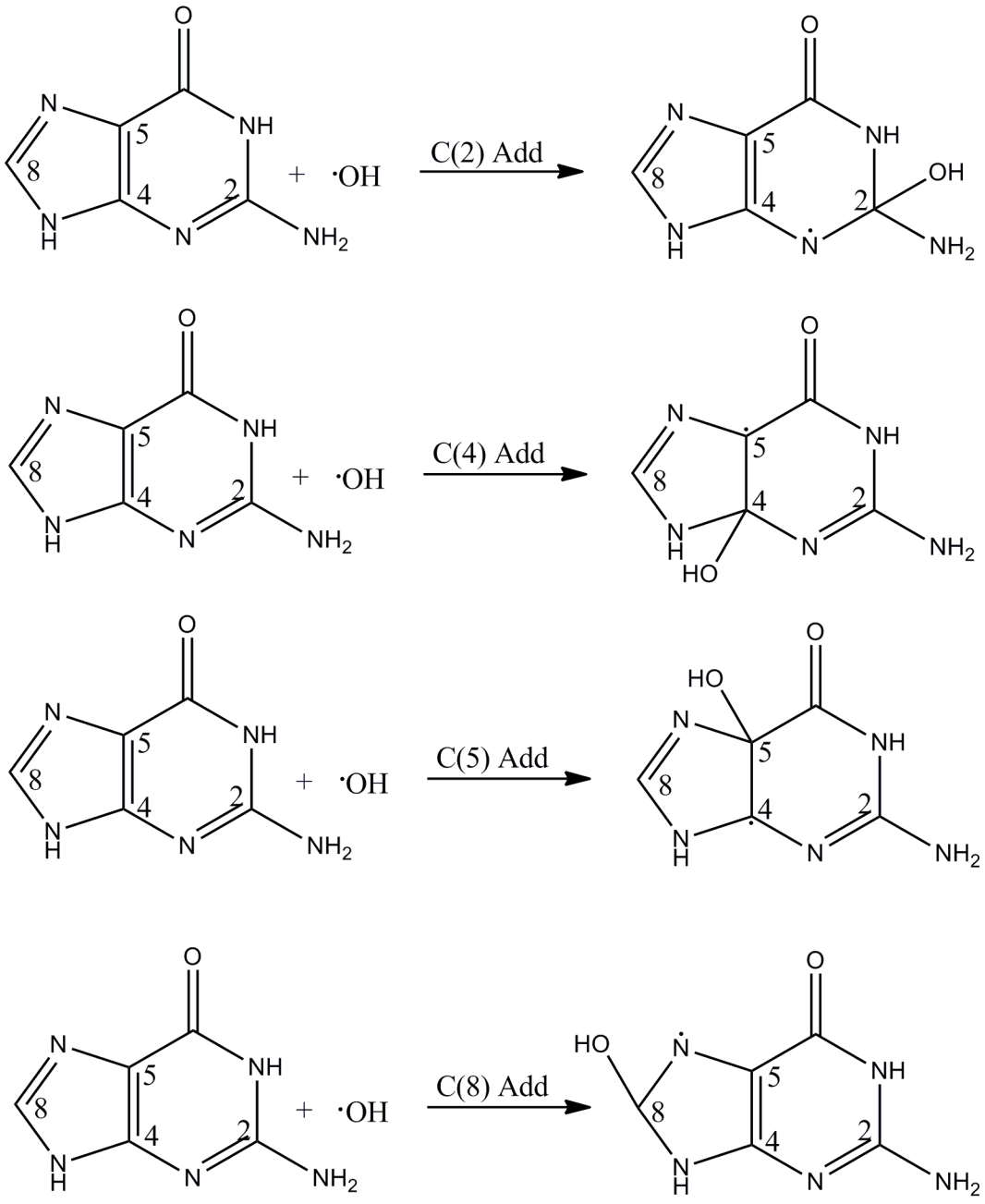

Figure 4: Hydroxyl radical addition to the guanine base

Theoretical

Previous work on $OH^{\cdot}$ Addition to bases has primarily focus on the geometry and hyperfine coupling constants of oxidation products [25] with some work done on the thermodynamics of $OH^{\cdot}$ addition to Thymine and on the C(4) and C(8) positions on Guanine. The results of the Thymine and Guanine thermodynamics [15,16] study were used to check the approach used in this paper. The thymine study showed reaction free energy of -56.4 kJ mol^{-1} for C(5) addition and -74.7kJ mol^{-1} for C(6). As is seen, these free energy calculations do not match up with the results of experimental work. More on this will be discussed later. For the Guanine study, free energies of -7.53 kJ mol^{-1} for C(4) and -21.68 kJ mol^{-1} for C(8) were found [27]. Once again this does not agree with experiment. Both the thymine and guanine study were done using B3LYP/6-31G** on Gaussian 98.

Table 2: Table from Aydogan [4] showing the results of monte carlo simulation of hydroxyl radical attack on the Guanine and Adenine moieties of DNA Bases, Nucleotides, single base pairs and 38-bp DNA

	Guanine				Adenine			
	C2	C4	C5	C8	C2	C4	C5	C8
Free bases	22	32	28	18	29	24	33	14
Nucleotide	30	28	25	17	30	22	36	16
Single base pair	34	29	21	16	33	14	38	15
38-bp DNA without steric hindrance	27	32	22	19	37	12	44	7
38-bp DNA with steric hindrance	28	41	16	15	31	18	38	13
Experiments	10	60	5	25	25	25	25	25

[a] Percentage values are normalized to 100% for each moiety studied.

Recently, monte carlo methods were used to calculate percentages of $OH^{\cdot}$ addition to DNA strands and free bases [4] This was done using reaction rates to calculate the reaction radius for each base. The simulation was done then stepping an $OH^{\cdot}$ molecule and letting it add to a base when coming with the reaction radius of the base. This method used steric hindrance of surrounding, non-reacting atoms. The results are reproduced here in Tables 2 and 3. Here it is seen that only for Cytosine and

Guanine are the results similar to experiment, and only when steric hindrance of a 38-bp

Table 3: Table from Aydogan [4] showing the results of monte carlo simulation of hydroxyl radical attack on the Thymine and Cytosine moieties of DNA Bases, Nucleotides, single base pairs and 38-bp DNA

	Cytosine		Thymine		
	C5	C6	C5	C6	MH[b]
Free bases	39	61	39	24	37
Nucleotide	42	58	42	25	33
Single base pair	43	57	40	26	34
38-bp DNA without steric hindrance	35	65	37	39	24
38-bp DNA with steric hindrance	42	58	48	25	27
Experiments	87	13	60	35	5

[a] Percentage values are normalized to 100% for each moiety studied.
[b] Methyl hydrogens.

DNA strand is used. It is obvious then, that more information must be taken into account than just the rate of reaction and steric hindrance. To count for the electrophilic nature of the hydroxyl radical, the reaction radius' were scaled based on the partial charge of the reacting atom based on electrostatic potential calculations of Hobza and Sponer [26] shown in Table 4. However, in this a strange number was used for the C(5) position of Adenine and Guanine. In the papers cited by Aydogan as a reference for the partial

Table 4: Partial charges calculated at the MP2/6-31G* level by Hobza and Sponer

EP Partial Charge		
	Cytosine	Thymine
C(5)	-0.653	0.055
C(6)	0.207	-0.059
	Adenine	Guanine
C(2)	0.452	0.841
C(4)	0.538	0.394
C(5)	0.013	0.051
C(6)	0.277	0.236

charges used, neither C(5) values match and are much lower than what is stated. Therefore the scaled results will be ignored here.

Chapter Five

Results

Method and Materials

All calculations were performed using the Jaguar program by Schrodinger. Free bases and the $OH^{\cdot}$ radicals were created using the Maestro GUI also by Schrodinger with the OH radical being added to the bases site by site, each was run separately. DFT functionals B3LYP, BLYP and PBE0 were used for all calculations along with the 6-31G** basis set. Geometry optimizations and vibrational analyses were done on the $OH^{\cdot}$ and each base separately, then the free energies and entropies of a given base were added to the free energy and entropy of the $OH^{\cdot}$ molecule to obtain the total reactant value. Geometry optimizations and vibrational analysis were then done on the bases with the radical attached to a specific site to obtain the product free energies and entropies. The changes of the free energies and entropies were calculated between products and reactants to find the most thermodynamically favored sites.

Calculations were also performed on the free bases for HOMO's, Fukui indices and Mulliken population analysis. These calculations were done using the B3LYP functional and 6-31G** basis set, with the exception of one calculation for Thymine, this used the cc-pVTZ basis set as explained in the appropriate section. Again bases were created in Maestro and Jaguar was used to calculate the values. Solvation was performed on the bases as well to obtain the Electrostatic potential partial charge distribution. Jaguar uses the Poisson-Boltzmann continuum model for salvation (Tannor et al, Martin et al). Fukui indices were calculated by Jaguar using the methods given by Contreras et al and Chamorro et al. Both the radical and electrophilic Fukui indices are

given, but since $OH^{\cdot}$ is highly electrophilic, the electrophilic values of the Fukui indices are used. The graphical surfaces of the HOMO's are shown when necessary.

Thymine

Thermodynamic calculations were first done on thymine to test this method compared to the results of Wu, et. al. The results from the calculations for this paper are given in Table 5. From the results discussed previously, these show good agreement and the methods used for this paper are acceptable. The C(5) addition is the least

Table 5: Thermodynamic Quantities for Thymine given for various Functionals with the 6-31G basis set.**

Thymine Thermodynamic Quantities (kJ/mol)						
	ΔH			ΔG		
Atom	B3LYP	BLYP	PBE0	B3LYP	BLYP	PBE0
C(5)	-88.47	-93.44	-105.34	-47.37	-52.83	-64.2
C(6)	-114.2	-115.19	-131.62	-74.8	-76.24	-92.1

thermodynamically favorable site with a Gibbs energy of -47.37kJ mol^{-1} compared to -42.6kJ $mol^{-1}$from Wu, et al and C(6) is the more favorable with a Gibbs energy change of -74.8031 kJ mol^{-1} compared to -85.5kJ mol^{-1} from Wu, et al.

These results are in contrast to the experimental results which show a greater percentage of addition to the C(5) position rather than the C(6). From this, it can be concluded that the addition of the hydroxyl radical to the Thymine base is not a thermodynamically controlled reaction but rather a kinetically controlled reaction. Given

Table 6: Partial Charges of the reactive atoms in Thymine calculated with B3LYP/6-31G**

Thymine Partial Charges			
	Gas	H_2O	
Atom	Mull.	Mull.	EP
C(5)	0.0107	0.005	-0.056
C(4)	0.108	0.117	-0.0018

the high reaction rates of the hydroxyl radical with the DNA bases and the strong electrophillicity of the radical itself, the electronic structure of the bases should have great influence on the reaction path and site of addition. With this in mind, calculations to find the HOMO's (Highest Occupied Molecular Orbital), Fukui indices and partial charge from Mulliken populations were performed. The results from Mulliken partial charges (shown in Table 6) of Thymine match up well with the experimental results than did the thermodynamics. Shown in Figure 5 are the HOMO orbits. As can be seen, the larger orbit(and hence large HOMO value) can be seen centered on the C(5) atom, therefore

Table 7: Fukui indices for the thymine base calculated at the B3LYP/6-31G level**

Thymine Fukui Indices				
	Radical		Electrophilic	
Atom	Gas	H_2O	Gas	H_2O
C(5)	0.2385	0.2247	0.3277	0.3393
C(6)	0.263	0.2589	0.1483	0.1406

C(5) has the larger probability of an electron occupying that orbit and a greater chance of addition. The Mulliken population analysis was done in gas phase and in H_2O solvation. The results found here do not agree well with the MP2 calculations given by Hobza and Sponer discussed earlier. In both cases, they show that the C(6) atom is more negative atom and would therefore be the better site for radical addition. Because of this disagreement, further calculation was done using a larger basis set, cc-pVTZ to look at the effect of basis sets on the results. The use of cc-pVTZ/B3LYP did not change the ordering of the charge negativity. However, the charges were significantly lower with C(5) being -0.17643 and C(6) being 0.04182. These as well show that the C(5) position being the more negative and therefore more likely to attract an electrophilic radical. Lastly, the Fukui indices were calculated, the results are shown in Table 7 for both the radical and the electrophilic indices. The electrophilic indices show agreement with

experimental results while the radical indices do not. Given that the hydroxyl radical is highly electrophilic, it is reasonable to think that the electrophilic index would give a better description of the reaction path.

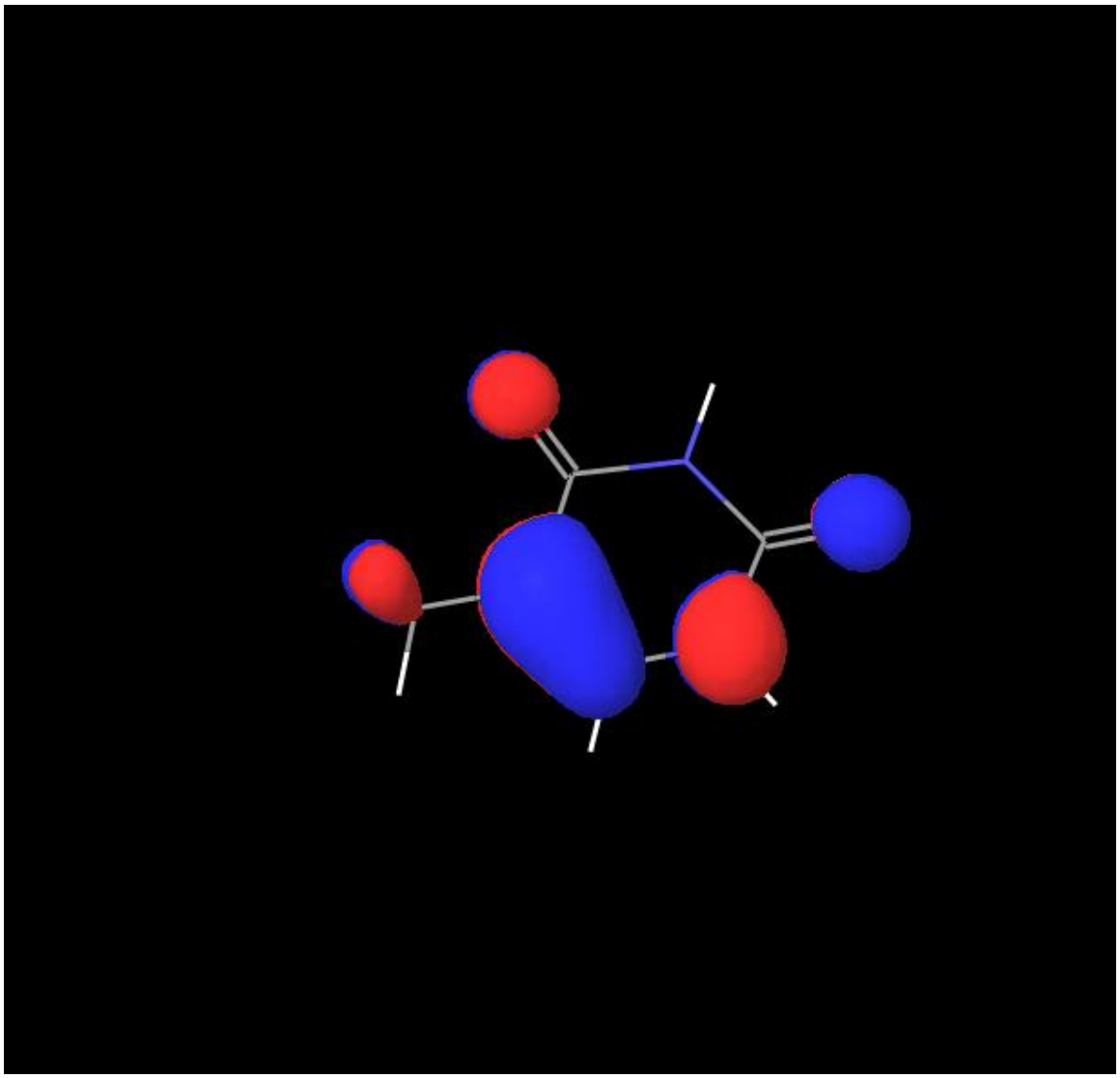

Figure 5: HOMO surfaces of the Thymine Base

Cytosine

Using the same process as with Thymine, the thermodynamics quantities were calculated for OH addition to cytosine. The results are shown in Table 8. Much like thymine, the Gibbs free energy does not match experimental results with C(6) being the most thermodynamically favored (-48.69 kJ mol^{-1}) and C(5) being the least (-46.45 kJ mol^{-1}). From the thermodynamic results, a more even distribution of attacks on each site

would be expected. Therefore, given the high disproportionality between the C(5) and C(6) sites in experimental results, 87% on C(5) and 13% on C(6), it can once again be concluded that these are kinetically controlled reactions.

Table 8: Thermodynamic quantities for the Cytosine base calculated for given functionals with the 6-31G basis set**

Cytosine Thermodynamic Quantities [kJ/mol]						
	ΔH			ΔG		
Atom	B3LYP	BLYP	PBE0	B3LYP	BLYP	PBE0
C(5)	-85.376	-94.02	-99.61	-46.45	-49.55	-61.43
C(6)	-87.8	-94.25	-99.52	-48.69	-54.6	-62.15

The study of the electronic structure of Cytosine, much like Thymine, matched up much better with the results. The HOMO orbit surface is shown in Figure 6. This is very similar to Thymine and the C(5) position again has the larger HOMO value. Notice t hat

Table 9: Partial charge for hydroxyl radical addition sites on the Cytosine base calculated at the B3LYP/6-31G level of theory**

Cytosine Partial Charges			
	Gas	H_2O	
atom	Mull.	Mull.	EP
C(5)	-0.1608	-0.171	-0.784
C(6)	0.168	0.166	0.357

qualitatively the C(5) surface is quite larger that the C(6). This could be interpreted as showing that a larger difference between the proportion of $OH^{\cdot}$ attack on C(5) to C(6) would be greater in cytosine compared to thymine, as the HOMO surface on C(5) is only

Table 10: Fukui indices of the Cytosine base calculated at the B3LYP/6-31G level**

Cytosine Fukui Indices				
	Radical		Electrophilic	
Atom	Gas	H_2O	Gas	H_2O
C(5)	0.1685	0.2128	0.2535	0.356
C(6)	0.2246	0.2374	0.0653	0.0905

slightly larger than C(6) in thymine. This trend was present in the Mulliken population analysis that was performed, Table 9. The partial charges for C(5) and C(6) show agreement with experiment and the difference between the charges are greater than in thymine. Also unlike thymine, the mulliken charge distribution agrees with the ordering given by Hobza and Sponer. The electrostatic potential calculated in H_2O however shows fairly good agreement in charge with Hobza and Sponers results, -0.207 for C(6) and .-0.653 for C(5). The radical Fukui indices indicate that C(5) is the less favorable position for addition, but the electrophilic indices show strong agreement with experiment, Table 10. From these results and the thymine results, it can be concluded that the addition of $OH^{\cdot}$ with pyrimidine bases follows a kinetically controlled, electrophilically favored reaction path.

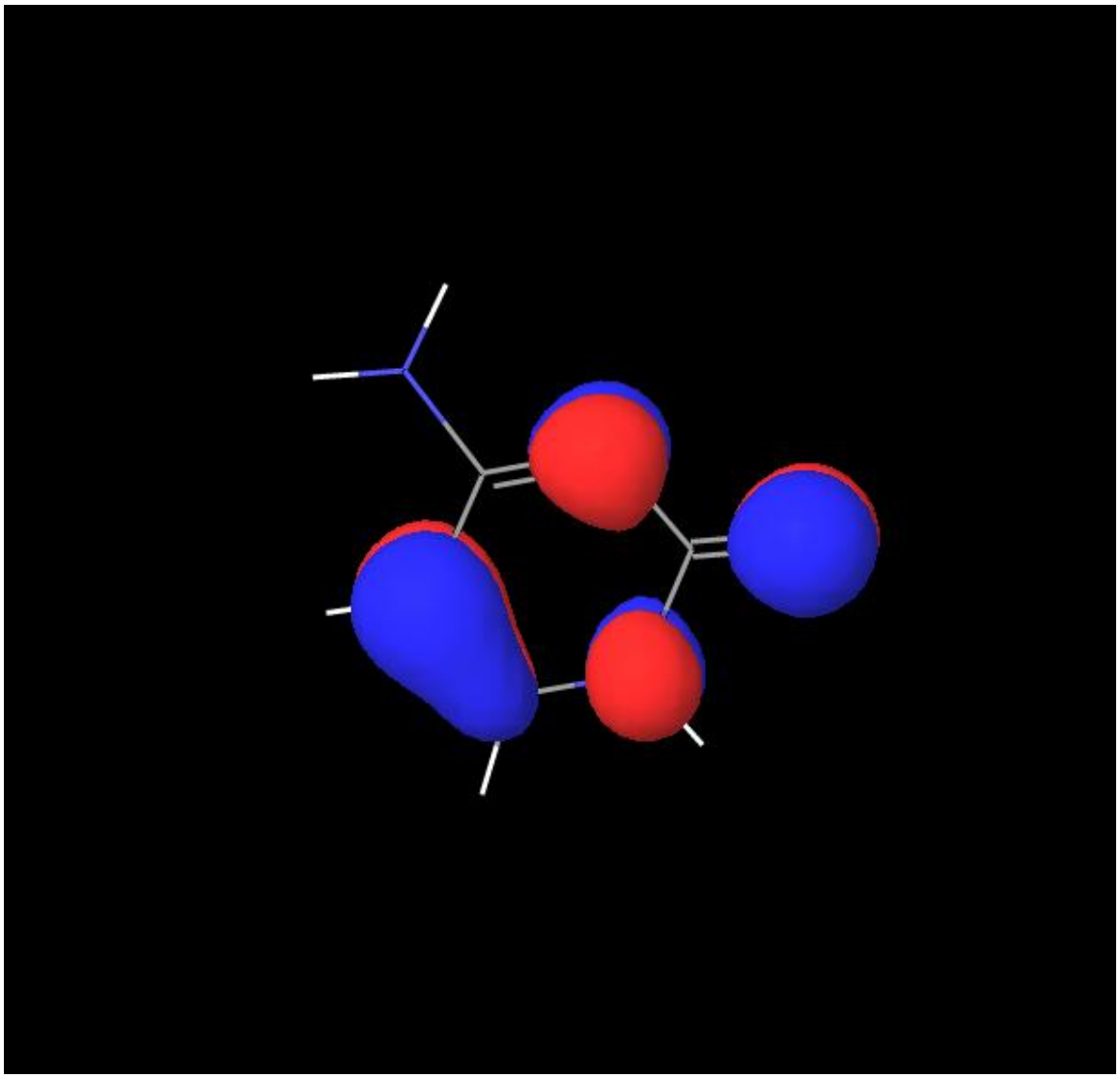

Figure 6: HOMO atom surfaces for the Cytosine base

Table 11: thermodynamic quantities for adenine calculated for various functionals with the 6-31G basis set**

Adenine Thermodynamic Quantities [kJ/mol]						
	ΔH			ΔG		
Atom	B3LYP	BLYP	PBE0	B3LYP	BLYP	PBE0
C(2)	-77.08	-90.39	-87.23	-36.42	-50.61	-45.74
C(4)	-48.51	-63.77	-59.53	-6.07	-21.7	-16.53
C(5)	-44.504	-61.72	-55.93	-2.576	-20.78	-13.206
C(8)	-135.52	-154.4	-146.25	-96.413	-113.56	-105.39

Adenine

From the results gained in this study, hydroxyl radical addition to the purine bases appear to be much more complex than addition to pyrimidines. The free energy results show very poor agreement with what was expected from experiment, Table 11. From experiment, C(4) shows the greatest percentage of addition, roughly 50%. However from the free energy calculations, addition to the C(4) has a free energy change of -6.07 kJ mol^{-1} and is one of the least favorable sites, only C(5) is less favorable which is in agreement with experiment as it has less than 5% addition. However, C(8) is the most favorable in terms of free energy, -96.413 kJ mol^{-1}. This reaction is seen in experiment at rate of around 37%. The C(2) position, which no data was found for experiment, is the second most favorable site with a free energy change of -36.42 kJ mol^{-1}. These results, much like with the pyrimidines, show that these $OH^{\cdot}$ addition must not be a thermodynamically controlled reaction.

Table 12: Partial charges for the adenine base calculated with B3LYP/6-31G for both gas and H_2O solvations**

Adenine Partial Charges			
	Gas	H_2O	
Atom	Mull.	Mull.	EP
C(2)	0.225	0.245	0.575
C(4)	0.504	0.52	0.66
C(5)	0.199	0.2	0.014
C(8)	0.285	0.3	0.367

The study of the electronic structure of Adenine does not seem to add much insight into the reaction process, unlike with the pyrimidines. In Figure 7, the result from the HOMO surface analysis is shown. It appears here, that the C(5) position has a greater HOMO coefficient and should be favored over the C(4), which is contrary to experiment. Also, it appears qualitatively here that C(5) may have a larger value than

Table 13: Fukui indices for the adenine base calculated with B3LYP/6-31G**

Adenine Fukui Indices				
	Radical		Electrophilic	
Atom	Gas	H_2O	Gas	H_2O
C(2)	0.1227	0.134	0.0678	0.0628
C(4)	0.03	0.0412	0.0547	0.0734
C(5)	0.1895	0.107	0.1588	0.1771
C(8)	0.18	0.1657	0.1208	0.1209

both C(8) and C(2), giving it preference over all sites in an elletrophilic reaction. The mulliken population analysis and electrostatic potentials give partial charges that also favor the C(5) position. As seen in Table 12, the partial charges do not match with experiment. Here, C(5) is shown to be the most negative (0.199*e* from mulliken in gas) with C(4) being the most positive (0.504*e* from mulliken in gas). Both C(2) and C(8) are in between with C(8) the more favorable. The ordering of these atoms does not change for Electrostatic Potential values, which match closely to the EP values from Hobza and Sponer. The Fukui indices fail to shed any light on the C(4)/C(5) favorability issue, Table 13. C(5) is favored over C(4) for both the radical(0.1895 for C(5) and 0.03 for C(4)) and the electrophilic (0.1588 for C(5) and .0547 for C(4)).

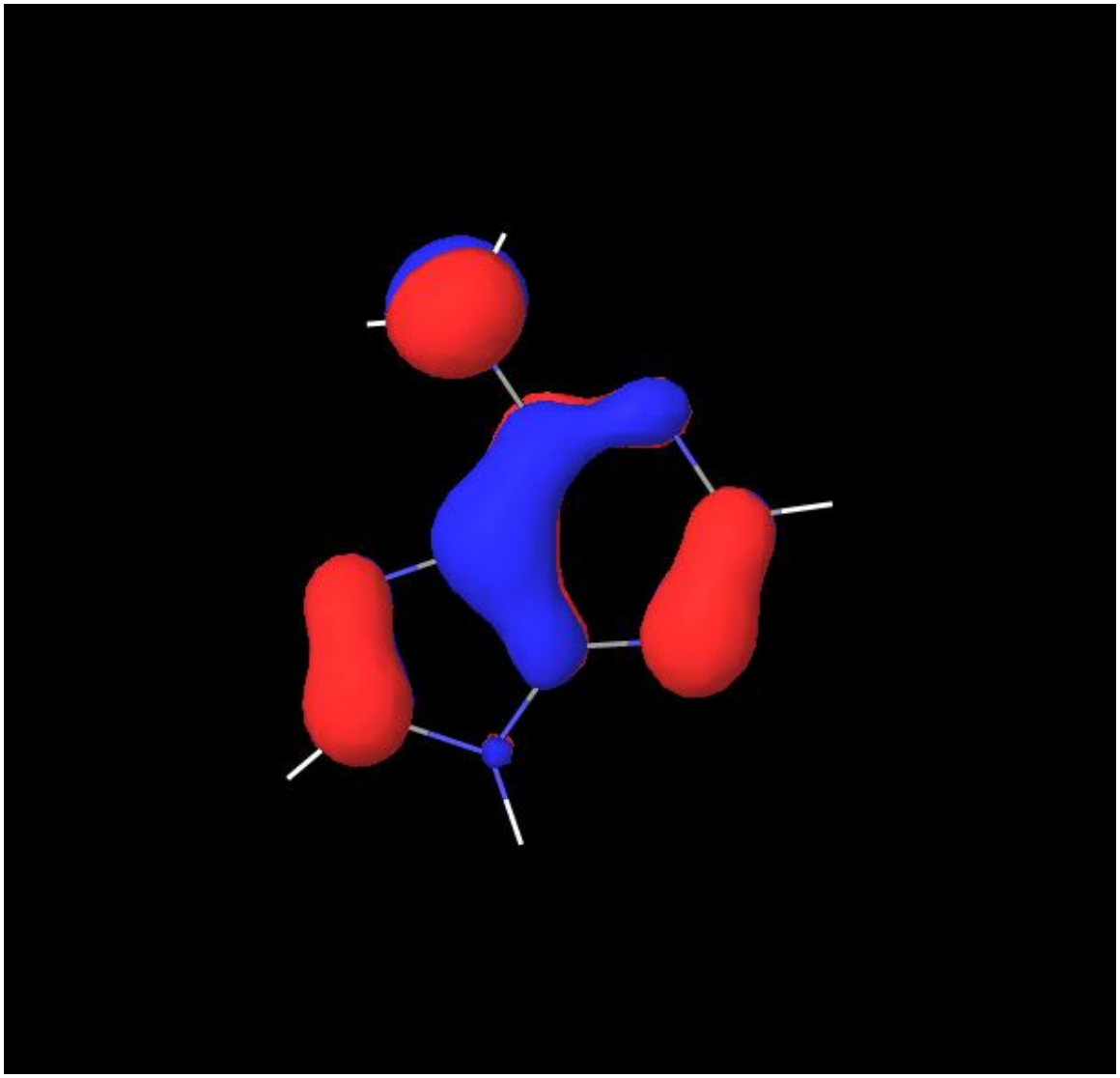

Figure 7: HOMO surface for the Adenine base calculated at B3LYP/6-31G**

Guanine

Guanine shows similar results to adenine. Thermodynamically, the C(8) position is the most favorable while C(5) is the least with C(2) being less favorable than C(4), Table 14. These again do not match what was expected from experiment, except for C(5) being the least favorable and all reactions being spontaneous. It is interesting to note the difference between the PBE0 results and the other two functionals. In the other

bases, the enthalpy and free energy results followed the ordering of the other two functional. However here, the ordering is very different. C(8) (-109.84 kJ mol^{-1}) is still the most stable addition site, but the C(5) (-64.16 kJ mol^{-1}) site becomes the second most favorable rather than the least and C(2) (-29.84 kJ mol^{-1}) becomes the least favorable. This is possibly just an anomaly of the PBE0 functional for guanine, as all calculations were checked for imaginary frequencies and the geometries were checked as well. From this data, the conclusion is that the addition of $OH^{\cdot}$ to the guanine base then is also kinetically controlled.

Table 14: Thermodynamic quantities of the Guanine base calculated for various functionals with the 6-31G basis set**

Guanine Thermodynamic Quantities [kJ/mol]						
	ΔH			ΔG		
Atom	B3LYP	BLYP	PBE0	B3LYP	BLYP	PBE0
C(2)	-90.19	-99.8	-71.37	-53.09	-61.67	-29.84
C(4)	-80.08	-89.93	-92.77	-37.69	-47.77	-49.81
C(5)	-59.88	-76.02	-106.62	-18.91	-35.25	-64.16
C(8)	-138.18	-148.84	-151.75	-98.45	-109.34	-109.84

The electronic analysis of guanine, much like with adenine, does not match with the experimental results. The HOMO surface is shown in Figure 8. This surface is similar to the adenine surface although the orbit around the C(6) atom is almost nonexistent. Seen in Table 15, the partial charges give C(5) as the most negative atom, 0.138. This is

Table 15: Partial charges for guanine calculated with B3LYP/6-31G**

Guanine Partial Charges			
	Gas	H_2O	
Atom	Mull.	Mull.	EP
C(2)	0.697	0.724	0.7599
C(4)	0.499	0.525	0.496
C(5)	0.138	0.13	0.1104
C(8)	0.277	0.284	0.3489

in contrast with experiment which shown very little C(5) addition, <5%. Unlike adenine, however, the C(4) atom is not the most positive. Here, the most positive atom is the C(2)

Table 16: Fukui indices for guanine calculated with B3LYP/6-31G**

Guanine Fukui Indices				
	Radical		Electrophilic	
Atom	Gas	H_2O	Gas	H_2O
C(2)		0.0237	0.174	0.0443
C(4)		0.1116	0.1109	0.088
C(5)		0.1237	0.2179	0.2222
C(8)		0.1395	0.0576	0.152

carbon. It is expected for this atom to not be a favored site of addition as it is only seen in 10% of addition products. C(4) though, is quite positive and is not what would be expected from experiment. The Fukui indices are similar to the partial charges and show no agreement in ordering with the experimental results, Table 16. C(5) is has the largest index for both the electrophilic index, 0.2179. In H_2O solvation, the atom with the largest radical index is the C(8) atom, 0.1395. (Note here that due to problems with the Trilobyte cluster, the nucleophilic indices were not recorded for gas phase and hence there is no radical index for the gas phase.) From these results, there is more work to be done on the purine bases.

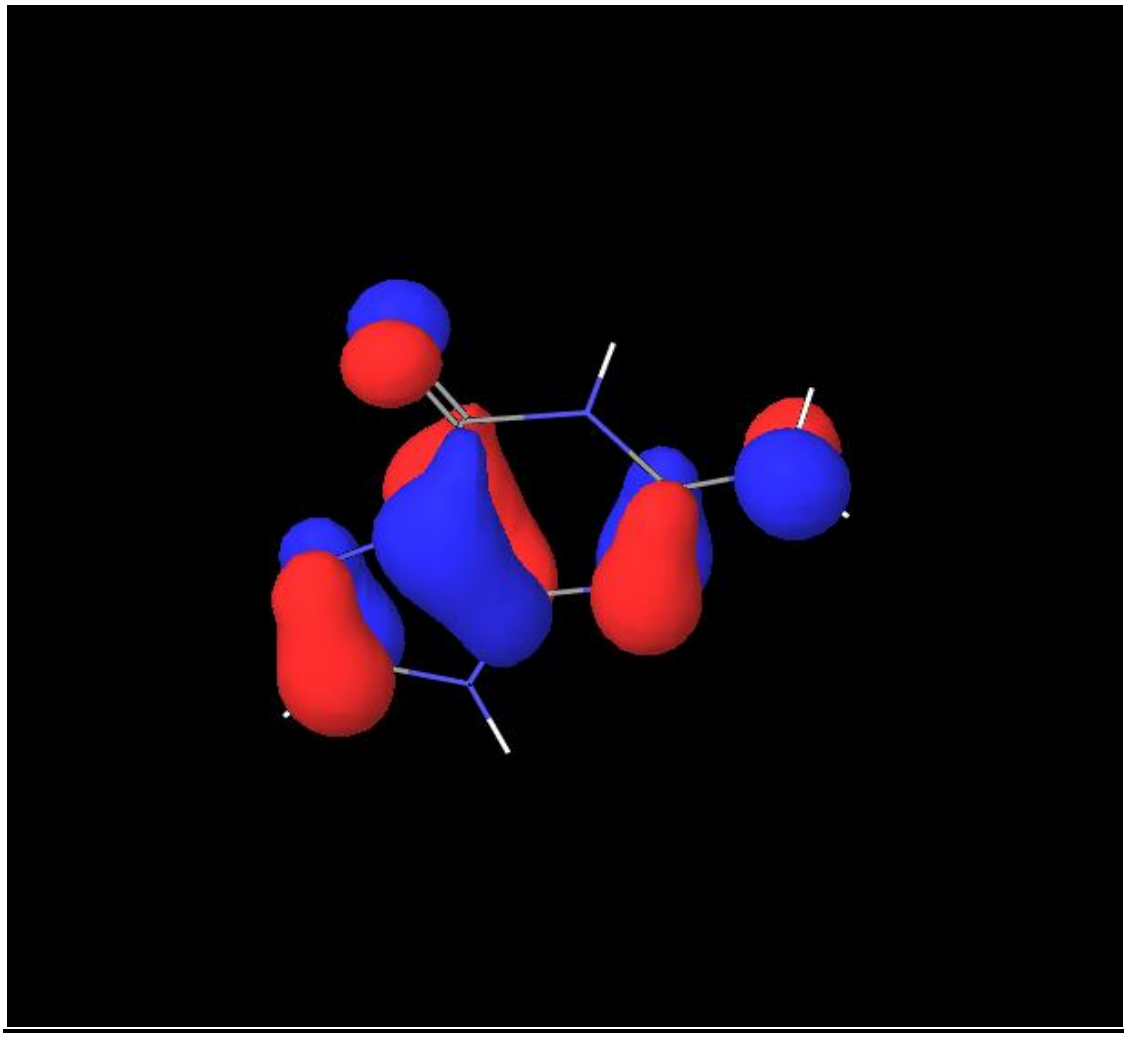

Figure 8: HOMO surface for guanine

Chapter Six

Discussion and Conclusion

The pyrimidine bases seem to be explained fairly well through the electrophilic nature of the hydroxyl radical. Experimental results match with the negativity of the reactive atoms in both bases as well as with the electrophilic Fukui indices and HOMO surfaces. Addition of this information to the studies of $OH^{\cdot}$ damage to DNA should provide useful information of the expected products. Of interest would be the application of this data to the monte carlo simulations performed by Aydogan. The results shown by Aydogan showed a poor match with experiment for the Thymine base because of the use of old EP charge calculations by Hobza, et all. Scaling the reaction radius using these results should provide with more similar results to experiment. It would also be interesting to see the results with a scaled radius based on the Fukui indices.

With the purine bases however, more work must be done. Neither thermodynamic or electronic analysis shows agreement with the experimental results. Perhaps calculating the thermodynamics free energy values with CCSD(T) and a large basis set will show that the C(5) (the shallowest change in energy) position may not be a spontaneous reaction, thereby explaining why that addition site is not seen. Also, calculations of the steric effects of the Methyl group and Oxygen atom have on the approach of the hydroxyl radical to the C(5) position need to be done. Transition state analysis would also be useful in the understanding of hydroxyl addition to the purine bases. Since the reaction is most kinetic, the free energy height of the transition state determines how fast the reaction occurs. The lower the lower the energy barrier, the faster the reaction and these the site with the lowest energy barrier would be the most preferential site for addition.

It is hoped that this information can lead to a better understanding of how radiation affects DNA at a molecular level. Looking at the favorability of addition sites, one could in theory, predict the percentage of damage product when a cell is irradiated by DNA. As each addition product affects the DNA strand differently and the proximity of damage products to each other will also determine how the products affect the strand as a whole, single strand and double strand breaks will be dependent on these damage products and their abundance after irradiation. Therefore, it is expected that there should be correlation between the percent addition of OH to sites and the number of single strand and double strand breaks. For example, if OH radical addition to any site of guanine causes a break in that backbone of the DNA strand, then another OH addition to a close by guanine (within a few base pairs) on the opposite backbone should results in a double strand break. However, it should not be assumed that addition to each site will result in a strand breaking addition product. Study needs to be done on which sites will result in a addition product that will in turn, break the DNA strand. That information, in association with the data provided here, could provide a better model of the amount of single strand and double strand breaks created through irradiation.

References

1. T. Douki, et al, Hydroxyl radicals are involved in the oxidation of isolated and cellular DNA bases by 5-aminolevulinic acid. *FEBS Lett.* **428**, 93-96 (1998)
2. J. Cadet, et al; Hydroxyl radicals and DNA base damage. *Mutat. Res.* **424**, 9-21 (1999)
3. B. Aydogan, et al; Site-specific OH attack to the sugar moiety of DNA: a comparison of experimental data and computational simulation. *Radiation Res.* **157**, 38-44 (2002)
4. B. Aydogan, et al; Monte Carlo simulation of site-specific radical attack to DNA bases. *Radiation Res.* **169**, 223-231 (2008)
5. A.D. Becke; Density-functional thermochemistry. III. The role of exact exchange *J.Chem.Phys*. 98 (1993) 5648-5652
6. C. Lee, W. Yang, R.G. Parr； Development of the Colle-Salvetti correlation-energy formula into a functional of the electron density, Phys. Rev. B 37 (1988) 785-78
7. C. Adamo, V. Baron, J Chem Phys **110**, 6158 (1999)
8. F. Jensen, *Introduction to Compuational Chemistry,* 2nd Edition Wiley and sons 2008
9. R. R. Contreras, et al; A direct evaluation of regional Fukui functions in molecules. *Chem Phys Lett* **304** 405-413 (1999)
10. E. Chamorro, P Perez; Condensed-to-atom electronic Fukui functions within the framework of spin-polarized density-functional theory. *Journal Chem Phys* **123**, 114107 (2005)
11. C. von Sonntag; *Free-Radical-Induce DNA Damage and Its Repair: A Chemical Perspective*. Springer (2006)

12. S. Steeken; Purine bases, nucleosides and nucleotides: Aqueous Solution Redox Chemistry and Transformation Reactions of Their Radical Cations and e^- and OH Adducts. *Chem Rev.* **89**, 503-520 (1989)
13. B. Balasubramanian, et al; DNA strand breaking by the hydroxyl radical is governed by the accessible surface area if the hydrogen atoms of the DNA backbone. *Proc. Natl. Acad. Sci. USA* **95**, 9738-9743 (1998)
14. L. Ashton et al; Temperature dependence of the rate of the reaction of OH with some aromatic compound in aqueous solution. *J Chem Soc Faradat Trans.* **91**, 1631-1633 (1995)
15. Y. WU, et al; On the mechanism of OH radical induced DNA-base damage: A comparative quantum chemical and Car-Parrinello molecular dynamics study. *Journ Phys Chem A* **108**, 2922-2929 (2004)
16. Schulte-Frohlinde D, et al Electron spin resonance studies of reactions of OH and SO_4 radicals with DNA, polynucleotides, and single base model compounds: In Minisci F (ed) free radical in synthesis and biology. Hluwer, Dordrecht, pp 335-359
17. H Catteral et al An EPR study of the transfer of radical-induced damge from the base to sugar in nucleic acid components: relevance to the occurrence of strand-breakage. *J Chem Soc Perkin Trans* **2** 1379-1385
18. Harza and Steenken, Pattern of OH addition to Cytosine and 1-, 3-, 5- and 6-substituted cytosines. Electron transfer and dehydration reactions of the OH adducts. *J Am Chem Soc* **105**, 4380-4386 (1983)
19. P O'Neil Pulse radiolytic study of the interaction of thiols and ascorbate with OH-adducts of dGMP and dG. Implications for DNA repair processes. *Radiat Res* **96**, 198-210 (1983)

20. P O'Neil, Hydroxyl radical damage: Potential repair by sulphydryls, ascorbate and other antioxidants. *Life Chem Rep* **1**, 337-342 (1984)
21. P O'Neil, et al, Potential repair of free radical adducts of dGMP and dG by a series of reductants. A pulse radiolytic study. *Int J Radiat Biol* **52**, 577-587 (1985)
22. LP Candeias, et al Reaction of OH with guanine derivatives in aqueous solution: formation of two different redox-active OH-adduct radicals and their unimolecular transformation reactions. Properties of G(-H)$^{\cdot}$ Chem Eur J **6**, 475-484
23. AJSC Viera, et al, Hydroxyl radical induced damage to the purine bases of DNA: in vitro studies. *J Chim Phys* **90**, 881-897 (1993)
24. AJSC Viera and S Steeken Pattern of OH radical reaction with N^6,N^6,9-trimethyladenosine. Production of three isomeric OH adducts and their dehydration and ring opening reactions. *J Am Chem Soc* **112**, 6986-6994 (1990)
25. SD Wetmore, et al Radiation products of Thymine, 1-Methylthymine, and Uracil Investigated by Density Functional Theory. *J. Phys Chem B* **102**, 5369-5377 (1998)
26. Hobza and Sponer, Structure, energetics, and dynamics of the nucleic base pairs: nonemperical ab intio calculations. *Chem Review*. 99 3247-3276 (1999)
27. C. J. Mundy, et al; Irradiated Guanine: A Car-Parrinello molecular dynamics study of dehydrogenation in the presence of an OH radical. *J Phys Chem A* **106**, 10063-10071 (2002)